

# MODELING THE TIME VARIABILITY OF BLACK HOLE CANDIDATES

*Light Curves, PSD, Lags*

D. KAZANAS

*Laboratory for High Energy Astrophysics*

*NASA/GSFC, Code 661 Greenbelt, MD 20771*

**Abstract.** We present a model for the aperiodic variability of accreting Black Hole Candidates (BHC) along with model light curves. According to the model this variability is the combined outcome of random (Poisson) injection of soft photons near the center of an extended *inhomogeneous* distribution of hot electrons (similar to those advocated by the ADAF or ADIOS flows) and the stochastic nature of Compton scattering which converts these soft photons into the observed high energy radiation. Thus, the timing properties (PSD, lags, coherence) of the BHC light curves reflect, to a large extent, the properties of the scattering medium (which in this approximation acts as a combination of a *linear* amplifier/filter) and they can be used to probe its structure, most notably the density profile of the scattering medium. The model accounts well for the observed PSDs and lags and also the reduction in the RMS variability and the increase in the characteristic PSD frequencies with increasing source luminosity. The electron density profiles obtained to date are consistent mainly with those of ADIOS but also with pure ADAF flows.

## 1. Introduction

The study of the physics of accretion powered sources, whether on galactic (X-ray binaries) or extragalactic systems (AGN), involves length scales much too small to be resolved by current technology. As such, this study is conducted mainly through the theoretical interpretation of their spectral and temporal properties. Until recently studies of this class of objects focused, for technical mainly reasons, on their X-ray spectra. These are generally fit very well with those of Comptonization of soft photons by hot ( $T_e \lesssim 10^9$  K) electrons, a process explored in great depth over the past

twenty or so years ([11]; R. Sunyaev this volume). Because the electron temperatures of matter accreting onto a black hole are expected to be similar to those necessary to produce the observed spectra, it has been considered that detailed spectral fits of these sources would lead to insights on the dynamics of accretion onto the compact object.

However, the determination of accretion dynamics requires the knowledge of the density and size of the emitting region, neither of which is provided by radiative transfer and spectral fitting considerations (the equations of radiative transfer involve the optical depth as the independent variable). Indeed, as shown explicitly in [6] and [5], plasmas of very different radial extent and density profiles can yield identical Comptonization spectra. The degeneracy of this situation can be lifted with the additional information provided by timing observations.

The timing properties of BHC, however, suggest length scales inconsistent with the prevailing notion that the observed X-rays are emitted from a region of size a few Schwarzschild radii,  $R_S$ : The power spectra (PSD) of BHC exhibit most of their power at scales  $\sim 1$  s, far removed from the characteristic time scales associated with the dynamics in the vicinity of the black hole horizon,  $R_S/c \sim 10^{-3}$  s. Until recently rather little attention has been paid to this time scale discrepancy, generally attributed to the (unknown) mechanism “fueling” the black hole, presumably operating at much larger radii; rather, more attention was paid to the flicker noise-type ( $\propto f^{-1}$ ) PSDs of this class of sources. Novel insight into the variability properties were introduced by [8], who showed that both the magnitude and the Fourier period dependence of the lags in the X-ray light curves at two different energies was inconsistent with Comptonization by a plasma of size  $\sim$  a few  $R_S$ ; the magnitude of time lags ( $\sim 0.1$  s) suggested an emission region of much larger size, precluding thus an explanation of the observed PSDs due to a modulation of the accretion rate onto the black hole.

These discrepancies between the expected and the observed variability of GBHC led [6], [3], [5] and [7] to propose that, contrary to the prevailing notions, the size of the scattering region responsible for the X-ray emission is not  $R \simeq 3 - 10 R_S$  but rather  $R \gtrsim 10^3 R_S$ , as implied by the PSDs and lag observations. Furthermore, the scattering medium (corona) is *inhomogeneous*, with the electron density following the law,

$$n(r) = \begin{cases} n_1 & \text{for } r \leq r_1 \\ n_1(r_1/r)^p & \text{for } r_2 > r > r_1 \end{cases} \quad (1)$$

where  $r$  is the radial distance from the center of the corona (assumed to be spherical) and  $r_1$ ,  $r_2$  are its inner and outer radii respectively. The index  $p > 0$  is a free parameter whose value depends on the specific dynamical model that determines the electron density. For example, the ADAF of [10]

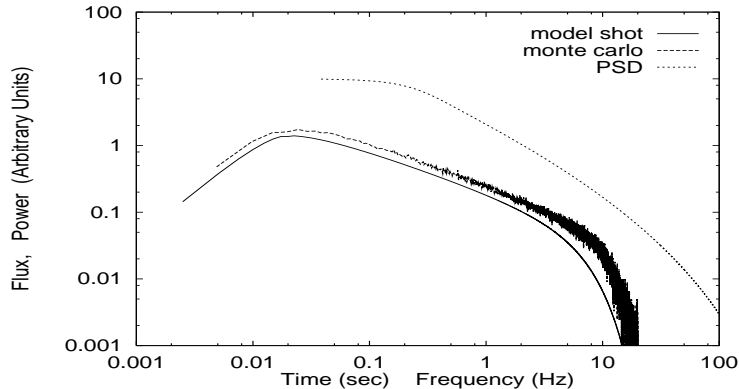


Figure 1. The response function  $g(t)$  of a corona with  $r_1 = 10^{-2}$  light s,  $r_2 = 10$  l. s,  $p = 1$ ,  $\tau_T = 1$ . The solid line is a fit to the MC data (dashed line). The dotted line is the Fourier spectrum  $|G(\omega)|^2$  of  $g(t)$ .

suggest  $p = 3/2$  and  $T_e \lesssim 10^9$  at radii as large as  $r \simeq (m_p/m_e)R_S$ , while models combining inflow and outflow [2], [1] (ADIOS) allow in addition values  $p \simeq 1$ . As pointed out in [6], [5] most of the data analyzed to date suggest  $p = 1$  with  $p = 3/2$  also acceptable in certain cases.

It is intuitively obvious that scattering in the extended configuration of Eq. (1) produces time lags over a range of Fourier periods similar to the range of radii span by the hot corona: Scattering at a given radius  $R$  increases the X-ray energy and introduces a lag  $\Delta t \lesssim R/c$  between the scattered and unscattered photons, the lag appearing at a Fourier period  $P = R/c$  ([5]; N. Kylafis these proceedings). To compare this to the lags given in [8] (which are the average over all such photon pairs scattered in a given decade in  $R$ , as a function of  $R$ ) one has to multiply  $\Delta t$  by the probability of scattering at a given radius,  $\mathcal{P}(R) \simeq \tau(R)$ , with  $\tau(R)$  the scattering depth over the radius  $R$ . For the density profile of Eq. (1),  $\tau(R) \propto R^{-p+1}$  and since the Fourier period  $P \propto R$ ,  $\langle \Delta t \rangle \propto R^{-p+2} \propto P^{-p+2}$ . Monte Carlo simulations and analytical considerations have shown that these arguments are essentially correct [5]. In addition, these simulations showed that the configuration of Eq. (1) produces light curves of high coherence over the range  $[r_2/c, r_1/c]$  of the Fourier period, provided that the soft photons are injected near its center.

## 2. The Model Light Curves

Based on these considerations one can easily produce model light curves, whose properties in the time or the Fourier domain can then be compared to observations for consistency. The high coherence of the observations [12]

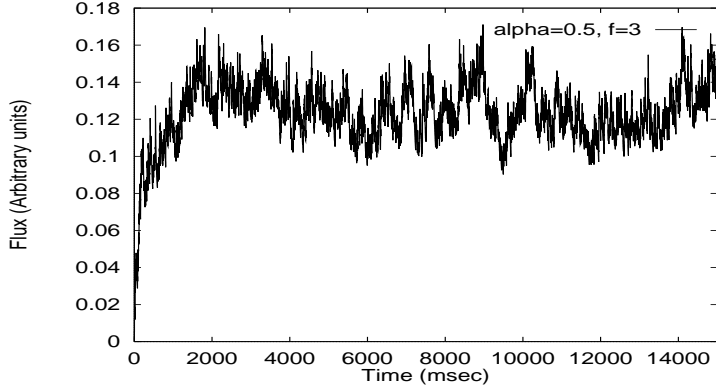


Figure 2. The light curve  $F(t)$  of Eq.(2) for the  $g(t)$  of Figure 2 and  $f = 3$ .

suggest injection of the soft photons at  $r \ll r_2$ . The response function,  $g(t)$ , of a corona with density profile given by Eq. (1) to an instantaneous release of soft photons at  $r \leq r_1$  has been computed by a Monte Carlo simulation [6], [7]. The result of a particular case is shown in Figure 1 along with an analytic fit. As pointed out in [5] these functions can be approximated well by a Gamma function distribution i.e.  $g(t) \propto t^{\alpha-1} e^{-t/\beta}$  ( $0 < \alpha < 1$ ,  $\beta > 0$ ).

Assuming linearity, i.e. that  $T_e$  is not affected by the photon flux, model light curves can be produced by an incoherent, random (Poisson) injection of shots of the form  $g(t)$ . The prescription for such a light curve is

$$F(t) = \sum_{i=1}^N Q_i \theta \left( t - \sum_{i=1}^N t_i \right) g(t - t_i) . \quad (2)$$

$Q_i$  are the shot amplitudes, assumed constant,  $\theta(t - t_1)$  is the Heaviside function and  $t_i$  is a collection of Poisson distributed time intervals obtained from the expression  $t_i = -f \cdot t_0 \cdot \log R_i$ ;  $R_i$  is a random number uniformly distributed between 0 and 1, and  $f$  is a real number, indicating the mean time between shots in terms of their rise time  $t_0$ . Figure 2 shows the light curve obtained using the above prescription with  $g(t)$  as given in Figure 1 and  $f = 3$ , while Figure 3 the light curve from an identical sequence of  $R_i$ 's and  $f = 10$ .

These light curves look similar to those of BHC sources in their low, hard state [9]. Due to the Poisson nature of  $t_i$ 's and the identical shape of the shots that make up these light curves, their PSDs are those of an individual shot, also shown in Figure 1 (dotted line). The form of the PSD is also quite similar to those of BHC (see [9]), with the high and low frequency breaks associated respectively with the inner  $r_1$  and outer  $r_2$  edges of the scattering corona.

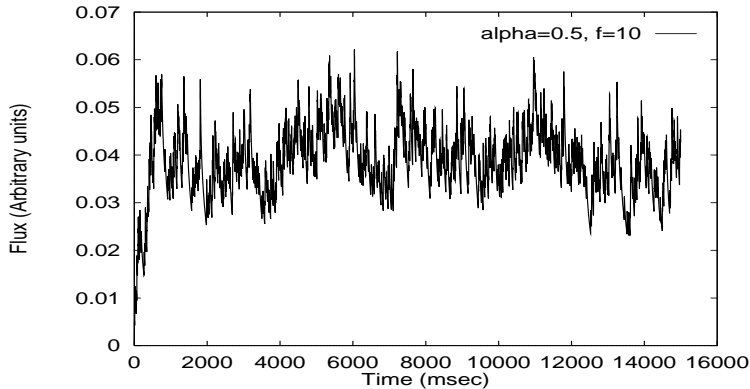


Figure 3. Same as Figure 2, with  $f = 10$ .

One can easily produce, in addition, light curves for different photon energies, considering that for photons of a higher energy,  $g(t)$  is approximately of the same form with only a small increase in the parameters  $\alpha$  and  $\beta$  [5]. While the resulting light curves are visually identical to those of lower energies, their difference is nonetheless easily seen in the phases of the corresponding FFT. We have generated this way model light curves appropriate to three different energies and then computed the corresponding pairs of phase lags (a)-(b), (a)-(c) as a function of the Fourier frequency measured in Hz; the results are shown in Figure 4. The phase lags as presented in this figure are very similar to those of the sources analyzed in [9] and in particular the X-ray transient GRO J0422+32 [4].

A correlation between the RMS variability and the value of  $f$  is the most prominent feature of Figures 2 and 3. Because, in the linear regime, smaller  $f$  is equivalent to higher luminosity (more photons per unit time), this correlation provides a natural account of the *observed* anticorrelation between the BHCs luminosity (in their hard spectral states) and their RMS variability. Furthermore, consideration of this model within its natural dynamic framework, namely that of ADAF, provides a direct correspondence between the dynamical and the timing properties of these systems: In ADAF all scales (and also  $r_1$  and  $r_2$ ) scale proportionally to  $v_{ff} \tau_{cool}$  with  $v_{ff}$  the free-fall velocity and  $\tau_{cool}$  the local cooling time. For  $\tau_{cool}$  inversely proportional to the local density (as is the case with ADAF), all length scales (and therefore frequencies) associated with the corona should depend on  $\dot{m}/\dot{m}_{Edd}$ , decreasing with increasing value of  $\dot{m}/\dot{m}_{Edd}$ ; hence the corresponding frequencies should increase with increasing luminosity, a behavior which has apparently been observed in most accreting sources (whether neutron stars or black holes).

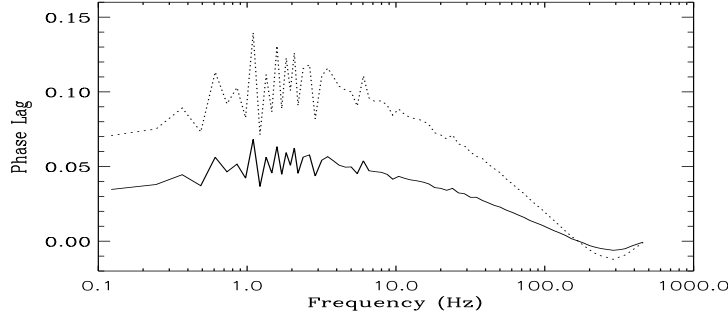


Figure 4. The phase lags of two sets of model light curves with the following parameters (a)  $\alpha = 0.5$ ,  $\beta = 16$  sec, (b)  $\alpha = 0.55$ ,  $\beta = 16$  sec, (c)  $\alpha = 0.6$ ,  $\beta = 16$  sec. The two curves correspond to the lags between: (a) - (b) (solid line) and (a) - (c) (dotted line).

### 3. Conclusions

(a) The model of the extended inhomogeneous corona provides in a simple, well understood fashion model light curves for BHC which have morphology, PSDs and phase (or time) lags very similar to those observed. (b) The dependence of the phase lags on Fourier period allows the determination of the density profile of the corona; the data are consistent both with  $p = 3/2$  (ADAF) and  $p = 1$  (ADIOS) flows. (c) The dependence of the RMS variability and the PSD break frequencies of BHC on their luminosity are also in general agreement with these dynamical considerations and provide a well defined framework within which these ideas could be tested through more detailed comparison with observations.

### References

1. Blandford, R. D. & Begelman, M. C. (1999), *MNRAS*, **303**, L1
2. Contopoulos, J. & Lovelace, R. V. E. (1994), *ApJ*, **429**, 139
3. Hua, X.-M., Kazanas, D. & Titarchuk, L. 1997a, *ApJ*, **482**, L57
4. Grove, J. E. *et al.* (1998), *ApJ*, **502**, L45
5. Hua, X.-M., Kazanas, D. & Cui, W. (1999) *ApJ*, **512**, 793
6. Kazanas, D., Hua, X.-M. & Titarchuk, L. (1997), *ApJ*, **480**, 735
7. Kazanas, D., Hua, X.-M. (1999), *ApJ*, **519**, 750
8. Miyamoto, S. et al. (1988), *Nature*, **336**, 450
9. Miyamoto, S. et al. (1992), *ApJL*, **391**, L21
10. Narayan, R. & Yi, I. (1994), *ApJ*, **428**, L13
11. Sunyaev, R. A. & Titarchuk, L. G., (1980), *A&A*, **86**, 121
12. Vaughan, B. A., & Nowak, M. A. (1997), *ApJ*, **474**, L43